



Effect of polytetrafluoroethylene-treatment and microporous layer-coating on the in-plane permeability of gas diffusion layers used in proton exchange membrane fuel cells

M.S. Ismail^{a,*}, T. Damjanovic^b, D.B. Ingham^a, L. Ma^a, M. Pourkashanian^{a,*}

^a Centre for Computational Fluid Dynamics, University of Leeds, Leeds LS2 9JT, UK

^b SGL Technologies GmbH, Meitingen 86405, Germany

ARTICLE INFO

Article history:

Received 7 March 2010

Accepted 10 April 2010

Available online 24 April 2010

Keywords:

PEM fuel cells

Gas diffusion layers

In-plane permeability

PTFE-treatment

MPL-coating

ABSTRACT

The in-plane permeability has been experimentally estimated for a number of carbon substrates and microporous layer (MPL)-coated gas diffusion layers (GDLs) as used in proton exchange membrane (PEM) fuel cells. The results show that the in-plane permeability of the tested carbon substrates decreases with increasing polytetrafluoroethylene (PTFE) loading and, in contrast, the greater is the PTFE loading in the MPL, the greater is the permeability. It has been shown that the in-plane permeability of the carbon substrates is reduced by an order of magnitude if they are coated with MPLs. Further, the permeability is different from one in-plane principal direction to another by a factor of about two. Finally, ignoring the inertial terms (for the reported flow rates) and the compressibility of the flowing air results in significant errors in the obtained values of the permeability.

© 2010 Elsevier B.V. All rights reserved.

1. Introduction

It is very crucial for the gas diffusion layer (GDL) in proton exchange membrane (PEM) fuel cells to have an appropriate permeability because it permits the reactant gases to efficiently reach the active sites in the catalyst layer. This in turn allows the electrochemical reactions, that are necessary to power the external loads, to proceed. Likewise, the GDL must be sufficiently permeable in order for it to transport the liquid water from the catalyst layer to the flow channels and vice versa and therefore control or eliminate the phenomena of flooding of the electrodes and/or dehydration of the membrane.

Typically, the properties of the GDL present a spatial anisotropy and this is due to the structure of the GDL that is characterised by a preferential orientation of carbon fibres in the in-plane directions. As such, the permeability, among other properties, is anisotropic, i.e. the permeability in one direction (e.g. the in-plane directions) is different to those in the other directions (e.g. the through-plane direction). Such a fact has motivated a number of research groups to estimate the permeability in two [1,2] and three [3] principal directions. However, most reported values of the permeability of the GDLs have been in the through-plane direction and this is mainly

because of the incorrect perception that the permeability of GDLs is isotropic, i.e. it is uniform in all directions. One more reason behind favouring such a measurement is that measuring the through-plane permeability is experimentally more easily performed [4]. However, Pharoah [4] showed that the pressure drop along the serpentine flow channels, the most commonly used flow-configuration, is much less sensitive to the through-plane permeability than to the in-plane permeability because the convective flow in these channels is mainly in the in-plane directions of the GDL.

Typically, GDLs (or simply carbon substrates) are treated with a hydrophobic agent, namely polytetrafluoroethylene (PTFE), in order to impart the hydrophobicity the GDLs require to remove the excessive liquid water from the porous electrodes. Further, the GDLs are normally coated with a thin layer, microporous layer (MPL), that consists of carbon powder and PTFE particles in order to enhance the contact between the GDL and the catalyst layer. Pharoah [4] suggested that adding the MPL to the carbon substrate does not alter the permeability of the latter layer in the in-plane direction as the convective flow, which is mainly in the in-plane direction, would be largely unaffected. However, he emphasised that it does reduce the through-plane permeability by up to four orders of magnitude. Thus, the convective flow is no longer significant in the through-plane direction as the respective permeability is normally lower than a computationally calculated threshold of $1 \times 10^{-13} \text{ m}^2$, which signifies the importance of the convection [4]. Therefore, it is clear that it is essential to estimate the in-plane permeability. It should be noted that some CFD modellers assume

* Corresponding authors. Tel.: +44 113 343 3824; fax: +44 113 246 7310.

E-mail addresses: pmmsai@leeds.ac.uk (M.S. Ismail), fue6mtz@leeds.ac.uk (M. Pourkashanian).

Nomenclature

A	constant coefficient, Pa
B	constant coefficient, s
K	permeability, m^2
L	thickness of porous medium, m
\dot{m}	mass flow rate, kg s^{-1}
m'	mass flux, $\text{kg}/(\text{m}^2 \text{ s})$
Mw	molecular weight, kg mol^{-1}
p	pressure, Pa
R	universal gas constant, $\text{J}/(\text{mol K})$
r	radius, m
T	temperature, K
t	time, s
V	volume, m^3
v'	non-dimensional velocity
V'	volume flux, $\text{m}^3/(\text{m}^2 \text{ s})$
v_0	reference velocity, m s^{-1}
v	velocity, m s^{-1}

Greek symbols

β	inertial coefficient, m^{-1}
μ	fluid viscosity, Pa s
ρ'	non-dimensional density
ρ_0	reference density, kg m^{-3}
ρ	density, kg m^{-3}

that the permeability is isotropic and it has the value of the highly reduced through-plane permeability of the MPL-coated GDLs. This would most likely result in an inaccurate prediction of the performance of the fuel cell as the in-plane permeability of the GDL has been significantly underestimated.

Now, we review some works whose authors have investigated the permeability in the in-plane directions. Feser et al. [5] found that the in-plane permeability of an MPL-coated GDL, TGP-60-H, is lower than the tested woven and non-woven tested carbon substrates by about an order of magnitude. This contradicts with the previously mentioned argument that the permeability in that direction would be largely unaltered [4]. Dhole et al. [6] found that the in-plane permeability increases with an increase in the PTFE loading in the MPLs. Likewise, Gurau et al. [1] showed that both the through- and in-plane permeabilities increase with an increase in the amount of PTFE in the MPLs. Ihonen et al. [2] found that the permeability of the tested carbon substrate in the in-plane direction is larger than that in the through-plane direction by a factor of about two. Also, they showed that the through-plane permeability of the MPL-coated GDLs may be smaller than that in the in-plane directions by two orders of magnitude. Further, Gostick et al. [3] measured the permeability of the GDLs in three principal directions and showed that most GDL samples present an anisotropic permeability even in the in-plane directions.

It should be noted that none of the above works have investigated the effect of PTFE loading in the carbon substrates on the in-plane permeability. Also, most of them ignored the effect of inertial pressure losses when calculating the permeability [2,5,6]. Further, the compressibility of the flowing gas has not been taken into account in most of the above-mentioned works [1,2,6] when estimating the in-plane permeability.

In this paper, which complements our previous papers on the through-plane permeability [7,8], the impact of PTFE loading in both the carbon substrates and the MPLs on the in-plane permeability has been investigated. Also, the anisotropy of the in-plane permeability, and its sensitivity to the compressibility of the flowing gas and to the inertial pressure losses have been probed. Further,

Table 1

Manufacturer's reported PTFE loading for carbon substrates.

GDL	PTFE loading, wt.%
SGL 10AA	0
SGL 10BA	5
SGL 10CA	10
SGL 10DA	20
SGL 10EA	30

Table 2

Manufacturer's reported PTFE loading for MPL-coated GDLs.

GDL	PTFE loading (MPL), wt.%
SGL 10BC	20–25
SGL 10BE	~50

light has been shed on the effect of MPL-coating on the in-plane permeability of the carbon substrates.

2. Materials and methods

2.1. Materials

The in-plane permeability was measured for five carbon substrates and two MPL-coated GDL samples. The samples were provided by SGL Technologies GmbH, Meitingen, Germany. The samples and their PTFE loading, as provided by the manufacturer, are listed in Tables 1 and 2, respectively.

2.2. Setup and procedures

The GDL sample (54 mm long \times 20 mm wide) is positioned between two steel plates as shown in Fig. 1. The sample is compressed by tightening the bolts. The thickness to which the GDL is compressed is controlled with the assistance of four feeler gauges. The flow rate of air was controlled and measured by a digital flow controller (Teledyne Hastings, HFC 202) that has a 0–101 min^{-1} range. The pressure drop across the sample was detected by a 0–50 psi differential pressure sensor, Omega PX 81D. The setup was gas sealed with an in-house gasket which is made by mixing two equal amounts of two chemicals, the first of which is the hardener and the second is the base (Jacobson Chemical Limited, Alton, UK). Prior to curing, the resulting mixture was spread all over the surface of the lower plate and then covered by the upper plate. The thickness of the gasket was controlled by feeler gauges. Once the mixture is between the plates, the setup was left intact for 2 days in order to allow the gasket to cure. It should be noted that the compressibility of the formed gasket is limited (50 μm or even less). Hence, two gaskets, with different initial thicknesses of 350 and 300 μm , were made so that the thicknesses to which the GDL samples are compressed, i.e. 340–270 μm , are covered. The gas seal of the setup was tested by pressurising the system to a high pressure (about 30 bar) for few hours and was found to be leak-proof. The GDL sample was placed carefully in the setup in a way that guarantees that there are no gaps between the GDL and the gasket, see Fig. 1b. The bolts were used to compress the GDL to four progressively decreasing thicknesses, namely 340, 320, 290, and 270 μm .

It has been noticed in the test that the more resistant to the flow is the GDL, the lower is the range of the flow rates to which the GDL samples are exposed. This is basically due to the limitation in the range of the used differential pressure sensor (maximum operating pressure is 50 psi). Therefore, the range of the flow rates under which the carbon substrates (more permeable) have been tested is considerably larger than that of the MPL-coated GDLs (less permeable), see Fig. 3 in Section 3.

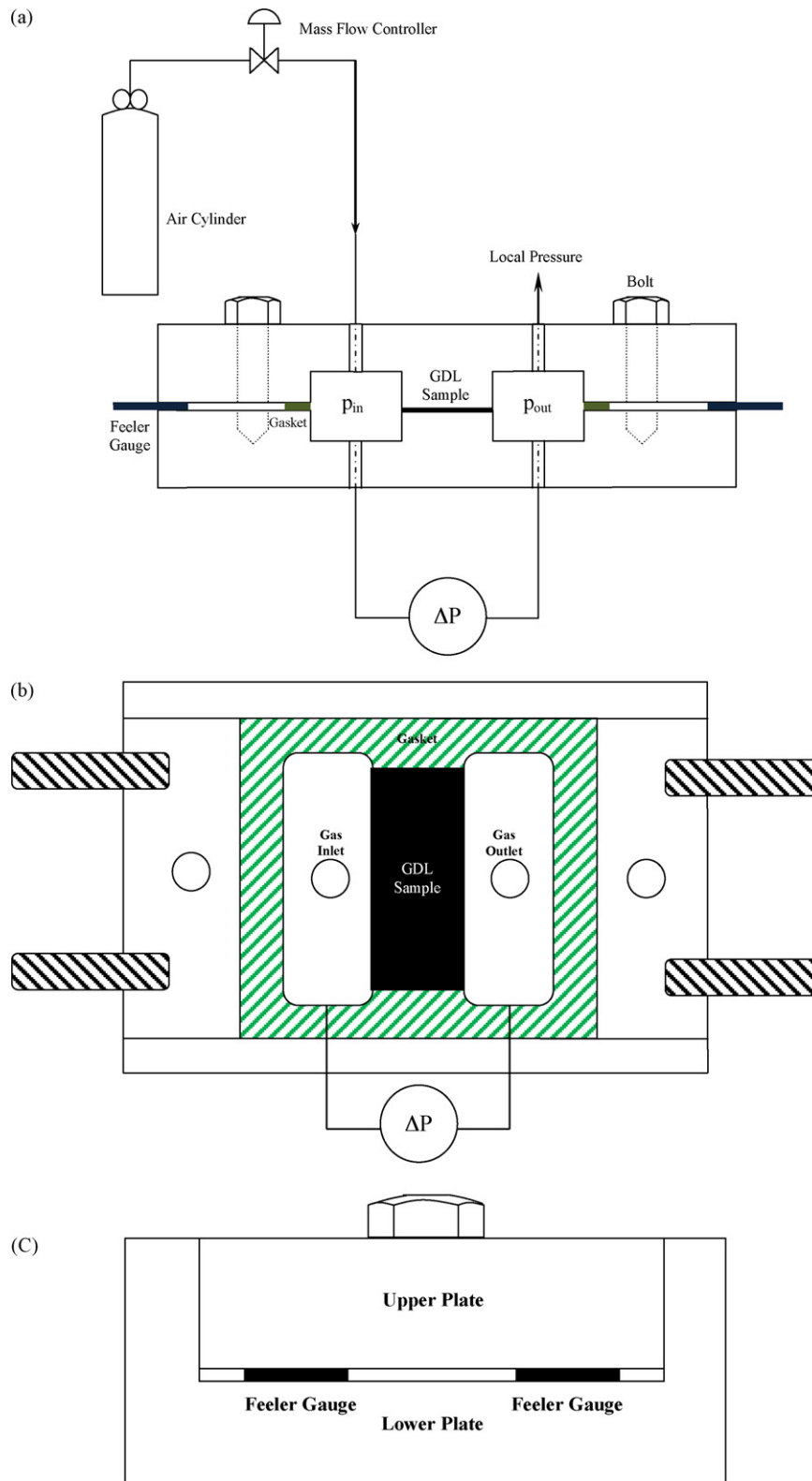


Fig. 1. A schematic diagram of the experimental setup: (a) front view, (b) top view, and (c) side view.

The present setup is similar to that developed by Gostick et al. [3]. However, two major modifications have been made to the latter setup. First, the number of the plates made was only two (lower and upper plates) rather than four (lower and upper plates plus two face plates) in order to minimise the possibility of air-leakage, see

Fig. 1c. Second, the inlet to and the outlet from the setup were positioned in the middle of the inlet and outlet gas chambers, rather than at their sides. This was done in order for the flowing gas not to have a preferential direction through the tested GDLs, see Fig. 1b.

2.3. Data analysis

The analysis of the data in this study is similar to that implemented in the through-plane permeability investigation [7,8]. The flow passing through the GDL sample is governed by Darcy's Law if it is creeping. Darcy's Law can be solved to yield [3,7,8]:

$$p_{in}^2 - p_{out}^2 = \frac{\mu}{K} \frac{2RTL}{Mw} m', \quad (1)$$

where p_{in} and p_{out} are the pressures before and after the GDL sample, μ and Mw are the viscosity and the molecular weight of air, respectively, K and L are the permeability and the thickness of the GDL sample, respectively, R is the universal gas constant, T is the temperature, and m' is the mass flux of air. If the velocity becomes relatively high, a modified form of Darcy's Law, normally termed as the Forchheimer Equation, should be considered. Likewise, solving the Forchheimer Equation leads to [3,7,8]:

$$p_{in}^2 - p_{out}^2 = \frac{\mu}{K} \frac{2RTL}{Mw} m' + \beta \frac{2RTL}{Mw} (m')^2 \quad (2)$$

where β is the inertial coefficient. The second term, non-Darcy term or inertial term, in the above equation corrects for the contribution of the inertial resistance to the pressure drop across the sample.

The in-plane permeability was estimated for two samples taken from each GDL material for each orthogonal direction, namely the direction parallel to the fibre orientation (designated for the sake of simplicity as 0°) and the direction normal to the fibre orientation (designated for the sake of simplicity as 90°).

As a way to validate the results obtained from the above setup, another setup that was originally designed to measure the permeability of normal fabrics used in textile industry has been employed to obtain the in-plane permeability for one of the GDLs being investigated in this study, namely SGL 10CA. More details on this setup is available in [9]. The GDL sample has been made annular, placed between two aluminium plates, and compressed with the assistance of a hydraulic press in such a way that air is forced to flow through the sample in the radial direction, see Fig. 2. It should be noted that the air cylinder was pressured to a certain level, namely 1 bar, and then it was allowed to leak out through the sample. The decay of the pressure with time was recorded using an appropriate oscilloscope.

The radius of the sample increases as the air flows towards its outer radius. Therefore, the form of the equation that governs the flow through the sample is different to that employed in the setup shown in Fig. 1. Now we present a rather detailed derivation whereby mathematical expressions for the in-plane permeability and the inertial coefficient can be obtained for the annular GDL samples. The flow of air through the GDL sample is given by Forchheimer Equation:

$$\frac{dp}{dr} = -\frac{\mu}{K} v - \beta \rho v^2 \quad (3)$$

where r is the radius of the GDL sample, ρ and v are the density and velocity of air, respectively. The rate of decrease in mass of air inside the cylinder, \dot{m} , is given by

$$\dot{m} = V \frac{d\rho}{dt} \quad (4)$$

where V is the volume of the cylinder and t is time. As air flows through the sample, the mass flow rate can be expressed as follows:

$$\dot{m} = 2\rho v \pi r L \quad (5)$$

Combining Eqs. (4) and (5) results in:

$$v = \frac{V}{2\pi L r \rho} \frac{d\rho}{dt} \quad (6)$$

The density of air can be obtained from the ideal gas law:

$$\rho = pD, \quad D = \frac{Mw}{RT} \quad (7)$$

Substituting Eq. (7) into Eq. (6) yields:

$$v = \frac{V}{2\pi L r p} \frac{dp}{dt} \quad (8)$$

The oscilloscope showed that the pressure of the system decays exponentially to zero, and thereby, the absolute pressure can be mathematically expressed as follows:

$$p = Ae^{-t/B} + p_a \quad (9)$$

where p_a is the ambient pressure, i.e. the pressure outside the system, and A and B are constant coefficients that have to be determined experimentally. Differentiating the above equation with respect to time results in:

$$\frac{dp}{dt} = -\frac{A}{B} e^{-t/B} \quad (10)$$

From Eqs. (8) and (10), one can obtain:

$$v = C \frac{1}{r} \frac{1}{p} e^{-t/B}, \quad C = \frac{A}{B} \frac{V}{2\pi L} \quad (11)$$

Substituting Eqs. (7) and (11) into Eq. (3) yields:

$$\frac{dp}{dr} = -\frac{\mu}{K} C \frac{1}{r} \frac{1}{p} e^{-t/B} - \beta C^2 \frac{1}{r^2} \frac{D}{p} e^{-2t/B} \quad (12)$$

Integrating Eq. (12) from p (at the inner radius r_i) to p_a (at the outer radius r_o) yields:

$$p^2 - p_a^2 = \frac{E}{K} e^{-t/B} + \beta F e^{-2t/B} \quad (13)$$

where

$$E = 2C\mu \ln(r_o/r_i), \quad F = 2C^2 D \left(\frac{1}{r_i} - \frac{1}{r_o} \right) \quad (14-15)$$

Eqs. (9) and (13) give:

$$2p_a A e^{-t/B} + A^2 e^{-2t/B} = \frac{E}{K} e^{-t/B} + \beta F e^{-2t/B} \quad (16)$$

Comparing the coefficients of $e^{-t/B}$ and $e^{-2t/B}$ results in mathematical expressions from which one can calculate the permeability and the inertial coefficient:

$$K = \frac{E}{2p_a A} = \frac{\mu V \ln(r_o/r_i)}{2\pi L p_a B} \quad (17)$$

$$\beta = \frac{A^2}{F} = \frac{2\pi^2 L^2 R T B^2}{V^2 M w ((1/r_i) - (1/r_o))} \quad (18)$$

3. Results and discussions

Fig. 3 presents the experimental results of the pressure gradient as a function of mass flux for one of the carbon substrates, SGL 10BA, and one of the MPL-coated GDLs, SGL 10BC, compressed to progressively four decreased thicknesses. It is clear that the pressure-dependency-on-the-flow-rate curves of the carbon substrate in two orthogonal in-plane directions, namely 0° and 90° , present a non-linearity, especially at the high flow rates. In contrast, the corresponding curves for the MPL-coated GDL display an apparent linear trend. The above two observations are applicable to the rest of the carbon substrates and MPL-coated GDLs being investigated in the present study. Initially, the inertial resistance to the flow of air was assumed to be significant and hence the Forchheimer Equation was used to estimate the permeability. The validity of this assumption is discussed in Section 3.4.

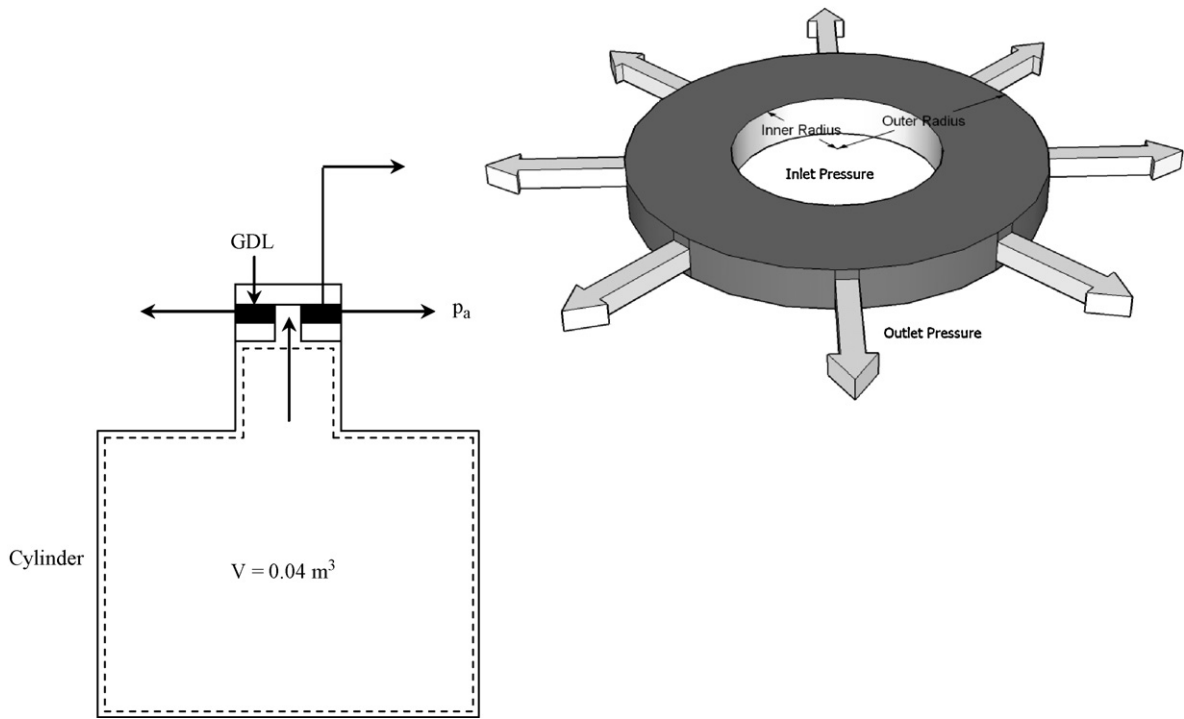


Fig. 2. A schematic diagram of the setup reported in [9]. The GDL sample is shown in the upper right corner.

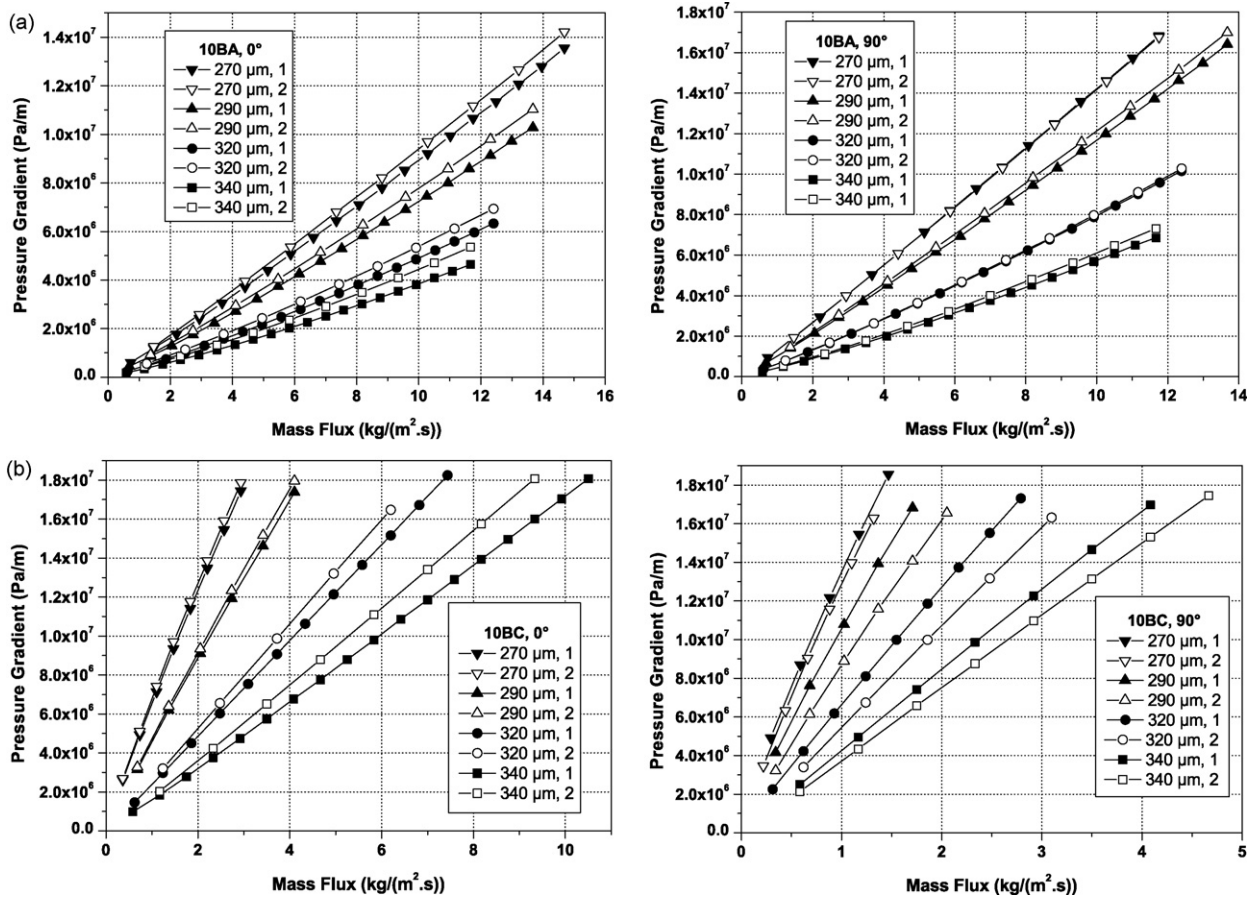


Fig. 3. Pressure gradient as a function of mass flux for (a) SGL 10BA, and (b) SGL 10BC. The angles (0° and 90°) and the numbers (1 and 2) in the legends represent the orientation of the fibres and the number of replica, respectively.

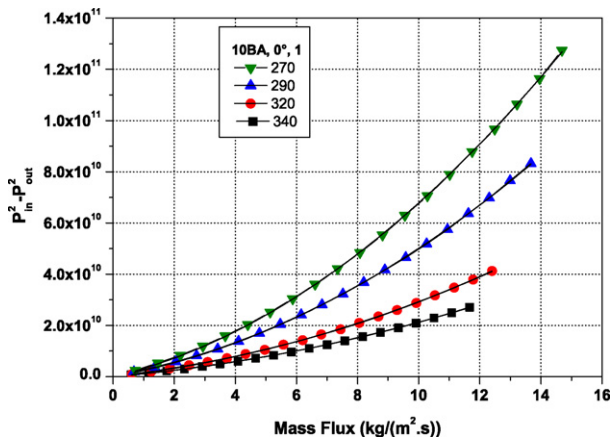


Fig. 4. Experimental results for $p_{in}^2 - p_{out}^2$ as a function of air mass flux for one of the tested carbon substrates, SGL 10BA.

3.1. Calculation of the permeability

The in-plane permeability K and the inertial coefficient β have been estimated by curve-fitting the experimental data for $p_{in}^2 - p_{out}^2$ as a function of mass flux m' to Eq. (2), see, as an example, Fig. 4.

Figs. 5 and 6 show the permeability and the inertial coefficient as a function of the compressed volume fraction, respectively. It appears that there have been very few works that have investigated the permeability of the GDLs being tested in this

study. Itonen et al. [2] estimated the in-plane permeability of the ‘uncompressed’ SGL 10BA and SGL 10BC to be 3.3×10^{-11} and $2.2 \times 10^{-11} \text{ m}^2$, respectively. They implicitly stated that the GDLs were compressed to a certain extent when they mentioned that the ‘real’ permeability values may be higher than the reported ones by about 30–50%. As the compressibility of the raw GDL is relatively high, the initial thickness (and in turn the permeability) of the GDL can be easily reduced with only a slight compression. As such, the comparison between the above-mentioned permeabilities and the present ones calculated for a compressed thickness of 340 μm (attained with a relatively slight compressive force) appears to be valid. The permeabilities for all the four SGL 10BA samples (two in 0° direction and two in 90° direction) were found to be between 4.16×10^{-11} and $6.23 \times 10^{-11} \text{ m}^2$, respectively. The permeability value obtained by Itonen’s et al. for SGL 10BA ($3.3 \times 10^{-11} \text{ m}^2$) is somewhat close to the lowest permeability measured for SGL 10BA, viz. $4.16 \times 10^{-11} \text{ m}^2$.

Likewise, the largest measured value for the permeability of SGL 10BC was $1.07 \times 10^{-11} \text{ m}^2$, which is lower than that reported by Itonen et al. [2] by a factor of about two. Such a discrepancy may be attributed to the fact that the initial thickness of SGL 10BC is relatively high when compared to that of SGL 10BA, viz. 420 μm , and therefore its ‘initial’ permeability would be considerably reduced when it is compressed to 340 μm . Bearing in mind that the permeability in one in-plane direction may be different to that in another direction by a factor of about two, see Section 3.3, Itonen et al. [2] did not mention the orientation of the fibres when they measured the in-plane permeability.

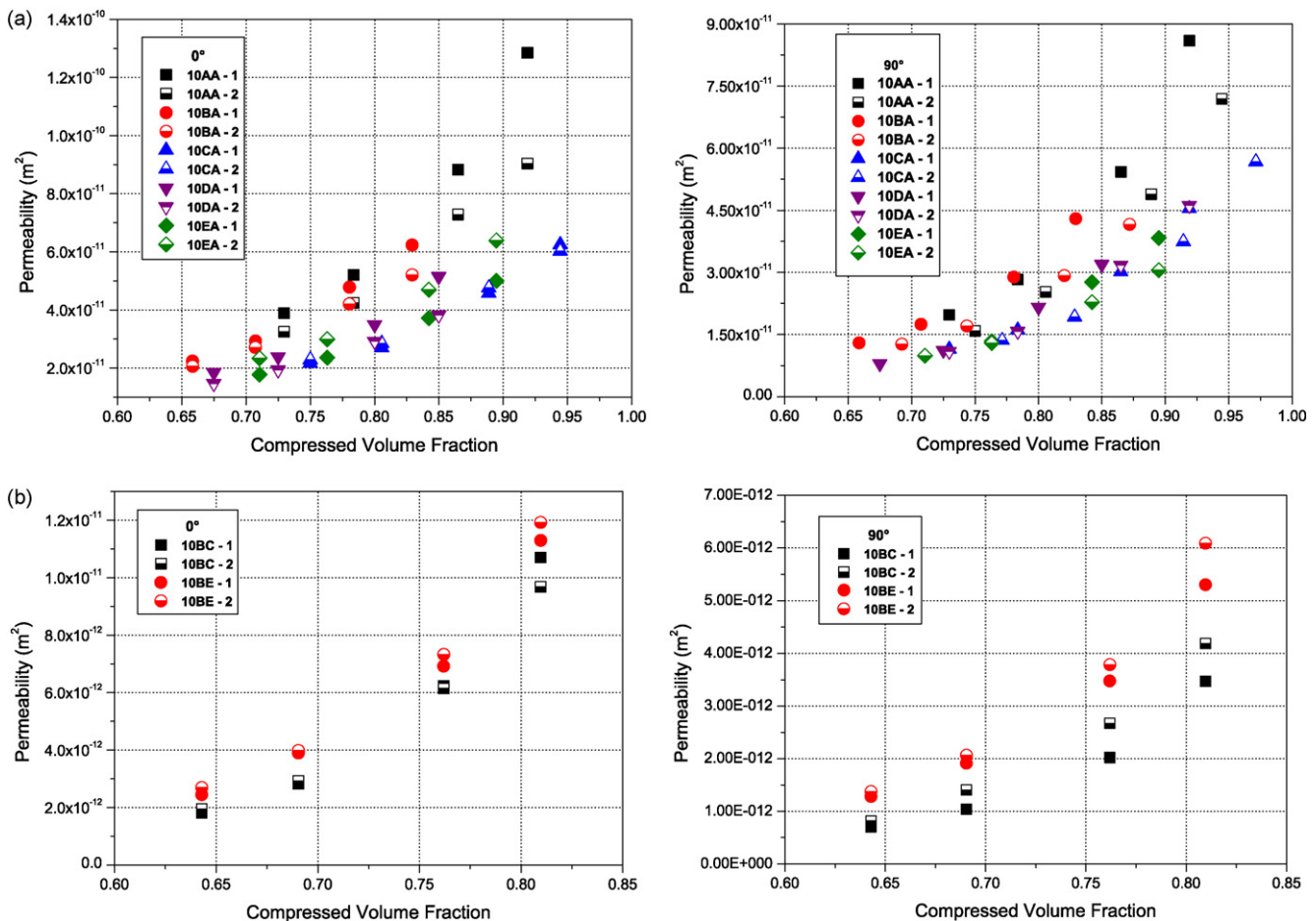


Fig. 5. The permeability as a function of compressed volume fraction for (a) the tested carbon substrates in 0° direction (left) and 90° direction (right), and (b) the tested MPL-coated GDLs in 0° direction (left) and 90° direction (right).

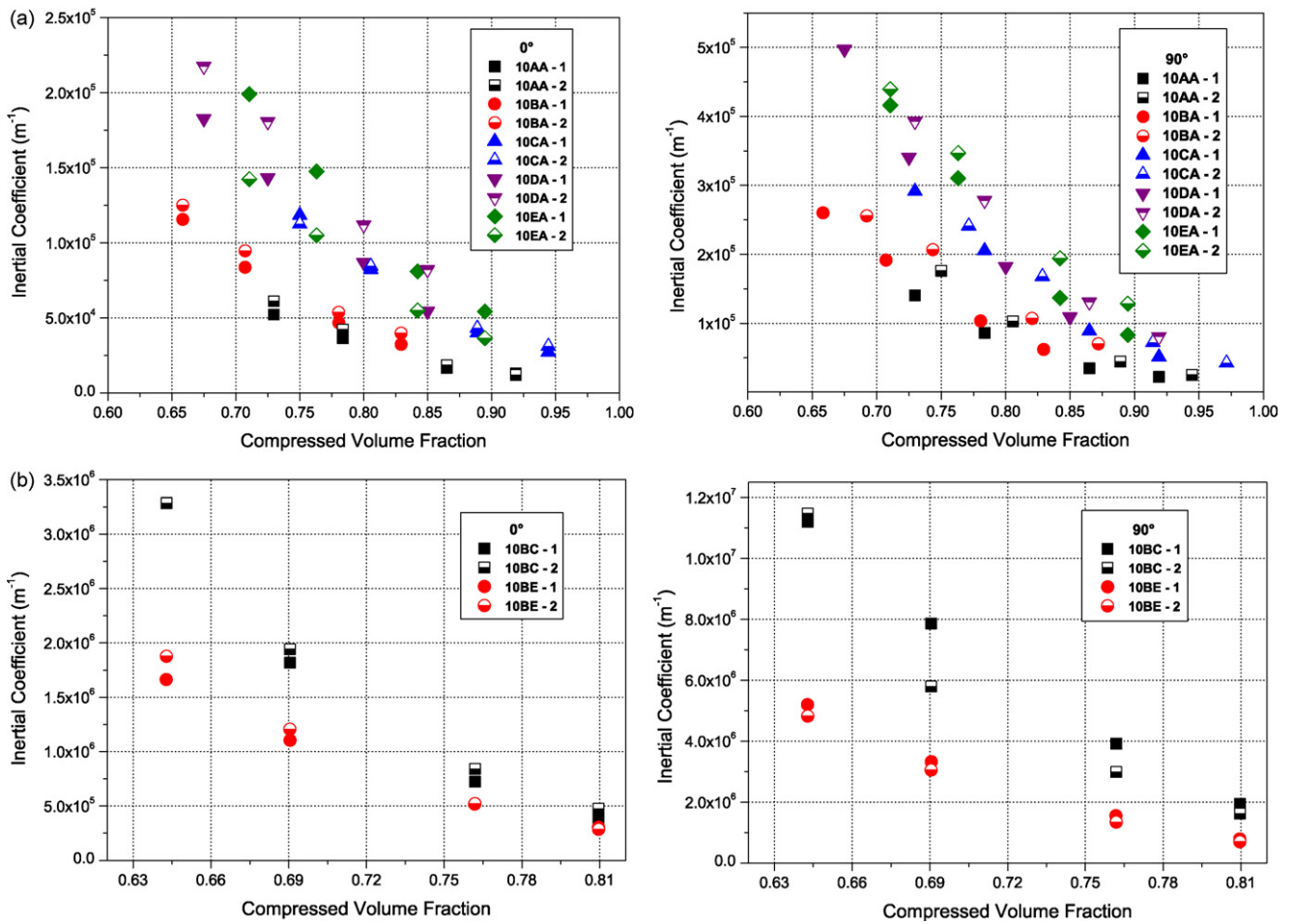


Fig. 6. The inertial coefficient as a function of compressed volume fraction for (a) the tested carbon substrates in 0° direction (left) and 90° direction (right), and (b) the tested MPL-coated GDLs in 0° direction (left) and 90° direction (right).

Gostick et al. [3] estimated the permeability of SGL 10BA in two in-plane orthogonal directions and found it to be between 2×10^{-11} and $5 \times 10^{-11} \text{ m}^2$ when compressed to about 85% of its initial thickness. This compares very well with the in-plane permeability of SGL 10BA reported in this study.

As mentioned in Section 2.3, the in-plane permeability of one of the GDLs being investigated, viz. SGL 10CA, was estimated using a setup that was basically fabricated to measure the permeability of normal fabrics [9]. Basically, the GDL sample was compressed between the two aluminium plates to a thickness of $340 \mu\text{m}$ with the assistance of a hydraulic press [9]. Feeler gauges were used to maintain the compressed thickness of the GDL, L . The cylinder was filled with air until it read 1 bar. Fig. 7 shows the experimental data for the pressure as a function of time after being curve-fitted. The resulting curve-fitting equation is given by $p = 1.153e^{(-t/98.99)} + p_a$.

As such, the coefficients A and B in Eqs. (17) and (18) are 1.153 bar and 98.99 s, respectively. The inner and outer radii (i.e. r_i and r_o) of the GDL sample were measured to be 1.5 and 3.5 cm, respectively, and the ambient pressure p_a was assumed to be atmospheric, viz. $1.013 \times 10^5 \text{ Pa}$. The viscosity of the air μ at normal conditions of pressure and temperature is about $1.86 \times 10^{-5} \text{ Pa s}$ and the volume of the cylinder V is 0.04 m^3 . Substituting the values of all these parameters into Eq. (17) results in the in-plane permeability K having the value of $2.94 \times 10^{-11} \text{ m}^2$. This result is in reasonable agreement to those estimated for the same GDL (at $340 \mu\text{m}$ thickness) using the setup shown in Fig. 1, namely 6.24×10^{-11} and $6.03 \times 10^{-11} \text{ m}^2$ (in 0° direc-

tion) and 5.67×10^{-11} and $4.53 \times 10^{-11} \text{ m}^2$ (in 90° direction), see Fig. 5a.

Likewise, the inertial coefficient β for SGL 10CA was calculated using Eq. (18) to be $3.14 \times 10^4 \text{ m}^{-1}$. It should be noted that the test was performed at a room temperature of $25 \text{ }^\circ\text{C}$. This result compares very well with the results shown in Fig. 6a as it lies between the reported limiting values for the inertial coefficient, namely 2.74×10^4 and $5.08 \times 10^4 \text{ m}^{-1}$.

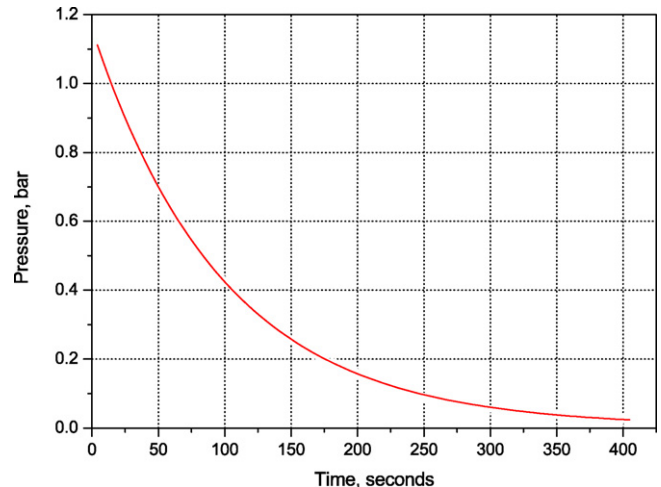


Fig. 7. Pressure decay curve for SGL 10CA compressed to $340 \mu\text{m}$.

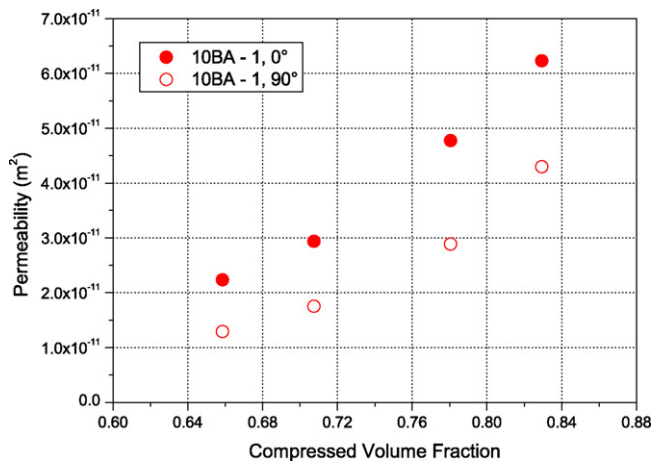


Fig. 8. The permeability as a function of compressed volume in two orthogonal in-plane directions, 0° and 90°, for SGL 10BA.

3.2. Effect of PTFE

It can be seen from Fig. 5a that the carbon substrates can be categorised into two groups, the first of which includes the untreated sample (SGL 10AA) plus the one that was slightly treated with PTFE, namely SGL 10BA (5% PTFE). The second group contains the rest of the carbon substrates that were treated with a considerably higher PTFE loading, viz. SGL 10CA, SGL 10DA, and SGL 10EA. This clustering rather reveals a relationship between the PTFE loading and the in-plane permeability: the greater is the PTFE loading, the smaller is the permeability in the in-plane directions. It is likely that the PTFE particles penetrate the pores existing between the carbon fibres and in turn reduce the porosity (and consequently the permeability) of the carbon substrates. In contrast, the MPL-coated GDLs present a different behaviour to that of the carbon substrates: the larger is the amount of PTFE in the MPLs, the larger is the in-plane permeability, see Fig. 5b. Similar observations have been reported and/or interpreted by [1,6,10]. Uchida et al. [10] studied carbon powder–PTFE mixtures and suggested that the large particles of PTFE could not penetrate the pores between the carbon grains (20–40 nm size) but do penetrate the pores between the larger-in-size carbon agglomerates (40–1000 nm size). This ultimately results in an increase in the size of the agglomerates and this in turn increases the size of the pores between them. In other words, the porosity, and consequently, the permeability of the carbon powder–PTFE mixtures increase with an increase in the PTFE loading. Apart from this and as expected, the permeability of the GDLs decreases with increasing compressive pressure as voids and air-gaps are closed up.

On the other hand, it appears that the effect of the compression and the PTFE loading on the inertial coefficient β is opposite to that on the in-plane permeability, see Fig. 6. In other words, the inertial coefficient (i) increases as the compression on the GDL increases, (ii) increases as the PTFE loading in the carbon substrates increases, and (iii) decreases as the PTFE loading in the MPLs increases. Apparently, both the PTFE loading and the increased compression increases the tortuous nature of the GDLs and accordingly increases the inertial resistance of the GDLs which manifests itself as an increase in the inertial coefficients.

3.3. Anisotropic in-plane permeability of GDLs

Fig. 8 shows the permeability in two orthogonal in-plane directions as a function of the compressed volume fraction for one of the GDLs tested in this study, namely SGL 10BA. It is clear that the in-

plane permeability in one in-plane direction (0° direction) is larger than that in the other direction (90° direction) by a factor of about two. As mentioned in Section 2, the fibres in the tested GDLs are preferentially oriented in one-plane direction, namely 0°. As such, the GDL is more permeable if the gas flows in a direction parallel to the 0° direction. On the other hand, the gas would experience a considerably higher resistance if it flows in a direction that is normal to the orientation of the fibres, 90° direction. This observation applies to all the other GDLs tested in the present study.

3.4. Effect of non-Darcy terms

To investigate the effect of the inclusion/exclusion of the inertial (or non-Darcy) terms, one should perform the non-dimensionalisation analysis whose details are available in [7,8]. The Darcy and non-Darcy terms are given as follows [7,8]:

$$\text{Darcy term} = \left[\frac{\mu}{K} v_0 \right] v' \quad (19)$$

$$\text{non-Darcy term} = [\beta \rho_0 v_0^2] \rho'(v')^2 \quad (20)$$

where v_0 and ρ_0 are the reference velocity and density of air, respectively, and v' , ρ' are the non-dimensionalised velocity and density, respectively. It should be noted that v' and $\rho'(v')^2$ terms are of order unity [7,8].

SGL 10BC in the 0° direction, whose pressure-dependency-on-the-flow-rate curve appears to be linear (as shown in Fig. 3b), was selected as an example in order to illustrate the importance of the non-Darcy term. Now we take the case at which the flow rate is the minimum reported one, i.e. 0.5 l min⁻¹ as the effects of the inertial pressure losses will be less profound. Therefore, if the non-Darcy term proves to be significant in this case, then its importance cannot be questioned in the other cases. The flow rate is $8.33 \times 10^{-6} \text{ m}^3 \text{ s}^{-1}$ and the cross-sectional area of the GDL sample is its length times the thickness to which the GDL is compressed. The latter parameter (i.e. the thickness) was selected to be the one at which the calculated inertial coefficient is the lowest, namely 340 μm . This gives a cross-sectional area and averaged air velocity of about $1.84 \times 10^{-5} \text{ m}^2$ and 0.45 m s^{-1} , respectively. The viscosity and the density of air at room temperature are $1.86 \times 10^{-5} \text{ Pa s}$ and 1.18 kg m^{-3} , respectively. The permeability K and the inertial coefficient β in this case were calculated to be $1.07 \times 10^{-11} \text{ m}^2$ and $3.79 \times 10^5 \text{ m}^{-1}$, respectively. Substituting all the above parameters into Eqs. (19) and (20) results in values of 7.82×10^5 for the Darcy term and 9.06×10^4 for the non-Darcy term. Dividing the latter term by the former one gives a number that has recently been termed as the Forchheimer number, Fo [3,11]. This number has a value of 0.11 in the above case. Thus, the error incurred by ignoring the inertial pressure losses, given by $E = (Fo/(1 + Fo)) \times 100$, is about 10%. This error is somewhat significant and cannot be overlooked. Therefore, one can envisage how important it is to include non-Darcy terms when calculating the in-plane permeability in the other cases (especially the ones at which the pressure dependency on the flow rate is clearly non-linear). For the above case (i.e. SGL 10BC in 0° direction), the error increases to about 65% at 8.5 l min⁻¹ flow rate. The above analysis has been conducted for the other GDL samples and similar results were obtained.

3.5. Effect of compressibility

If the compressibility of air is assumed to be negligible (i.e. the density of air is constant) then another simpler equation could be used to estimate the in-plane permeability [7,8]:

$$p_{\text{in}} - p_{\text{out}} = \frac{\mu L V'}{K} + \beta \rho L (V')^2 \quad (21)$$

Table 3

The calculated in-plane permeability for SGL 10BA using Eq. (2) (column 2) and Eq. (21) (column 3).

Thickness, μm	K (Eq. (2)) (10^{-11}) m^2	K (Eq. (21)) (10^{-11}) m^2	Error, %
340	6.23	4.93	20.81
320	4.78	3.69	22.67
290	2.94	2.28	22.58
270	2.24	1.76	21.09

where V is the volume flux. The resulting permeability values, using the above equation, suggest that it is underestimated by about 20%. SGL 10BA in the 0° direction was taken as an example, see Table 3. Similar results have been obtained for the other PTFE-treated GDLs.

However, the above finding was found to be unrelated to the MPL-coated GDL samples since Eq. (21) is not applicable to the respective pressure drop as a function of flow rates curves which have a linear trend, see Fig. 3b. It should be noted that a non-linear relationship has been revealed for the MPL-coated GDLs after fitting the experimental data of $p_{in}^2 - p_{out}^2$ as a function of flow rate to Eq. (2). However, using a differential pressure sensor with a higher range would allow higher flow rates to pass through the very resistant-to-flow MPL-coated GDL samples and then Eq. (21) may be applicable and in turn the underestimation of the permeability mentioned above may hold. Certainly this requires further experimental investigation.

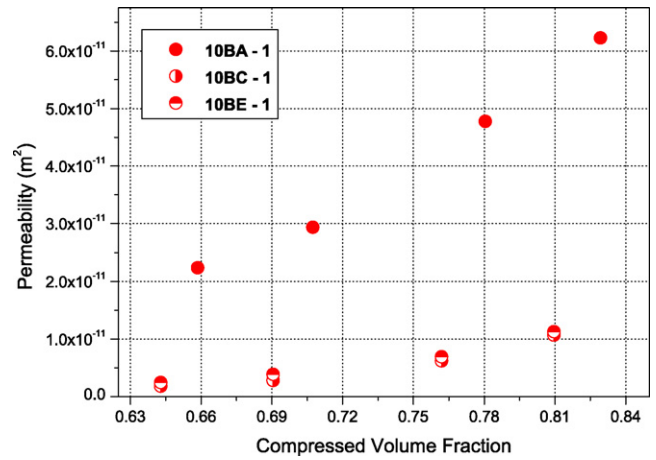


Fig. 9. The permeability as a function of compressed volume fraction for SGL 10BA after being coated with MPLs to form SGL 10BC and SGL 10BE.

3.6. Effect of MPL-coating

Undoubtedly, the MPL-coating reduces the through-plane permeability of the GDLs. As mentioned in Section 1, Pharoah [4] reported that the through-plane permeability of the carbon substrates may be reduced by up to four orders of magnitude if they are coated with MPLs.

Given that the MPL is in series with the carbon substrate, one may postulate that the in-plane permeability of the coated GDLs

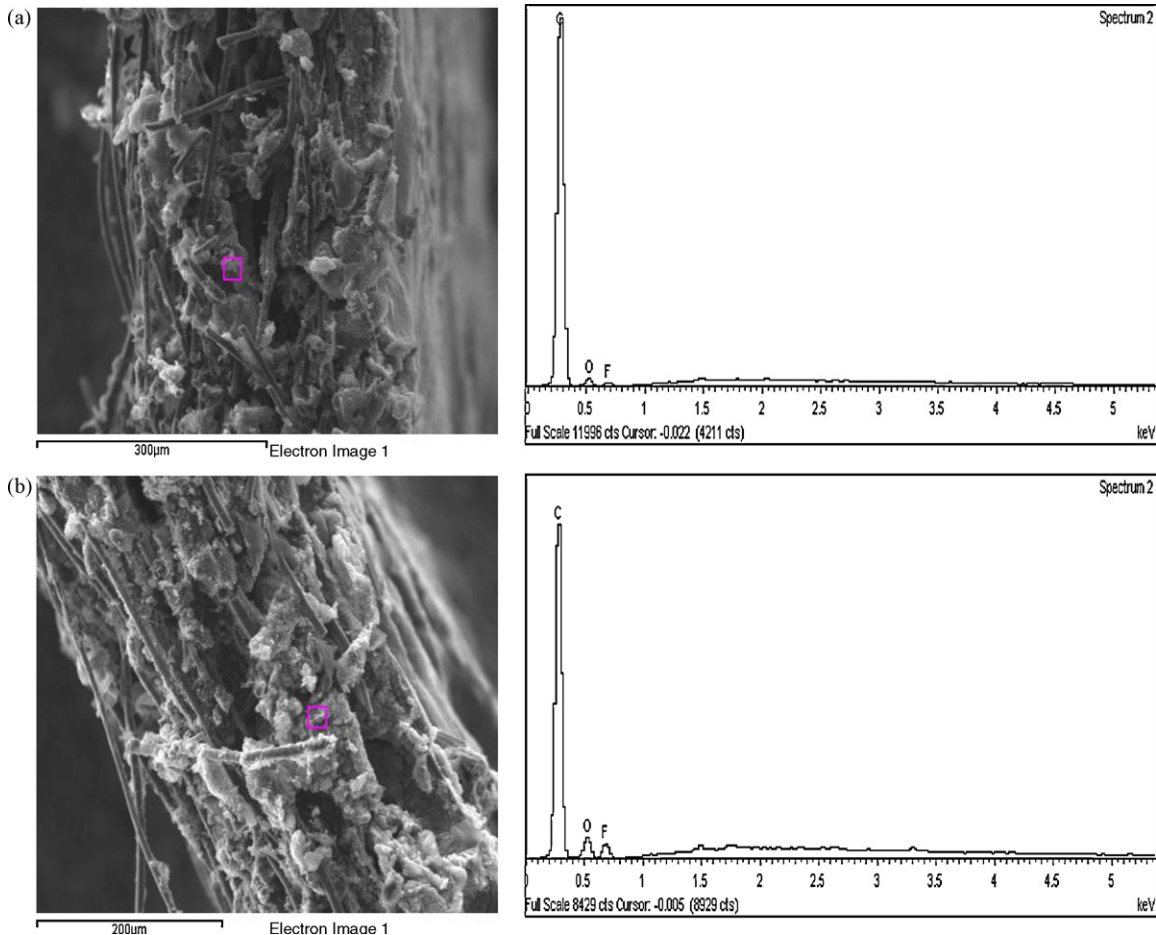


Fig. 10. EDX analysis for cross-sectional areas of (a) SGL 10BC and (b) SGL 10BE.

would not be affected as the body of the carbon substrate would remain unaltered [4]. However, Fig. 9 reveals that the in-plane permeability of the carbon substrate (SGL 10BA in this case) is reduced by an order of magnitude if it is coated with an MPL to form either SGL 10BC or SGL 10BE. Such a discrepancy could be attributed to the possibility that some MPL material has penetrated the structure of the carbon substrate and this in turn reduces the porosity of the latter layer and thereby imposes a higher resistance to the flow of air.

In order to investigate this argument experimentally, SEM images for the cross-sectional areas of SGL 10BC and SGL 10BE were taken, see Fig. 10. As suggested above, it appears from the images that some MPL material has migrated to the body of the carbon substrates (probably while applying the MPL to the carbon substrate). The composition of the presumably MPL clusters has been analysed with the assistance of energy dispersive X-ray (EDX) spectroscopy. The resulting spectra show clear fluorine peaks that signify the presence of one of the main constituents of the MPL material, PTFE, see Fig. 10. Therefore, the argument that the MPL material has penetrated the body of the carbon substrate and significantly reduced the in-plane permeability appears to be valid.

4. Conclusions

The in-plane permeability has been measured for some PTFE-treated carbon substrates and MPL-coated GDLs. The results show that the in-plane permeability for the tested carbon substrates decreases with an increase in the PTFE loading. In contrast, an increase in the PTFE loading in the microporous layers (MPLs) causes the in-plane permeability of the respective GDLs to increase. Interestingly, the effect of the PTFE loading on the inertial coefficient shows a completely opposite trend to that of the in-plane permeability.

The in-plane permeability of the tested GDLs is anisotropic as the in-plane permeability in one in-plane direction (parallel to the preferential orientation of the fibre) is greater than that in the other direction (normal to the preferential orientation of the fibres) by a factor of about two.

The exclusion of the non-Darcy terms, while solving for the in-plane permeability, results in a significant error, especially at

high flow rates. Likewise, neglecting the compressibility of air, when solving the Forchheimer Equation, introduces a considerable underestimation in the obtained in-plane permeability of the tested carbon substrates.

Finally, the perception that the MPL-coating has no effect on the in-plane permeability appears to be questionable as the in-plane permeability of the tested carbon substrates is reduced by an order of magnitude after MPL-coating.

Acknowledgments

The authors gratefully acknowledge financial support from a Dorothy Hodgkin Postgraduate Award, the UK Engineering and Physical Sciences Research Council (EPSRC), and Shell UK. Also, the authors would like to thank SGL Technologies GmbH, Germany, for providing the GDL sample materials. Deep gratitude is owed to Dr. Palitha Bandara, from School of Design, for constructive discussions and the use of his experimental facilities. The technical assistance of Mr. Paul Crosby for the experimental work carried out in this project is gratefully appreciated.

References

- [1] V. Gurau, M.J. Bluemle, E.S. De Castro, Y.M. Tsou, T.A. Zawodzinski, J.A. Mann, *J. Power Sources* 165 (2007) 793–802.
- [2] J. Itonen, M. Mikkola, G. Lindbergh, *J. Electrochem. Soc.* 151 (2004) A1152–A1161.
- [3] J.T. Gostick, M.W. Fowler, M.D. Pritzker, M.A. Ioannidis, L.M. Behra, *J. Power Sources* 162 (2006) 228–238.
- [4] J.G. Pharoah, *J. Power Sources* 144 (2005) 77–82.
- [5] J.P. Feser, A.K. Prasad, S.G. Advani, *J. Power Sources* 162 (2006) 1226–1231.
- [6] H. Dohle, R. Jung, N. Kimiaie, J. Mergel, M. Muller, *J. Power Sources* 124 (2003) 371–384.
- [7] M.S. Ismail, T. Damjanovic, D.B. Ingham, K. Hughes, L. Ma, M. Pourkashanian, M. Rosli, *J. Fuel Cell Sci. Technol.* 7 (2010) 1–7.
- [8] M. Ismail, K. Hughes, D. Ingham, L. Ma, M. Pourkashanian, M. Rosli, *Proceedings of the Seventh International Conference on Fuel Cell Science, Engineering, and Technology*, Los Angeles, 2009, pp. 713–721.
- [9] P. Bandara, C. Lawrence, M. Mahmoudi, *Meas. Sci. Technol.* 17 (2006) 2247–2255.
- [10] M. Uchida, Y. Aoyama, N. Eda, A. Ohta, *J. Electrochem. Soc.* 142 (1995) 4143–4149.
- [11] Z.W. Zeng, R. Grigg, *Transport Porous Media* 63 (2006) 57–69.